Marquette University

e-Publications@Marquette

Electrical and Computer Engineering Faculty Research and Publications

Electrical and Computer Engineering, Department of

9-21-2004

A Comparison of Micro-Switch Analytic, Finite element, and Experimental Results

Ronald A. Coutu Jr.
Marquette University, ronald.coutu@marquette.edu

P. E. Kladitis
Air Force Institute of Technology

Lavern A. Starman
Air Force Institute of Technology

J. R. Reid
Air Force Research Laboratory

Follow this and additional works at: https://epublications.marquette.edu/electric_fac

Part of the Computer Engineering Commons, and the Electrical and Computer Engineering Commons

Recommended Citation

Coutu, Ronald A. Jr.; Kladitis, P. E.; Starman, Lavern A.; and Reid, J. R., "A Comparison of Micro-Switch Analytic, Finite element, and Experimental Results" (2004). *Electrical and Computer Engineering Faculty Research and Publications*. 344.
https://epublications.marquette.edu/electric_fac/344

Marquette University

e-Publications@Marquette

Electrical and Computer Engineering Faculty Research and Publications/College of Engineering

***This paper is NOT THE PUBLISHED VERSION;* but the author's final, peer-reviewed manuscript.**
The published version may be accessed by following the link in the citation below.

Sensors and Actuators A: Physical, Vol. 115, No. 2-3, (September, 2004): 252-258. DOI. This article is © Elsevier and permission has been granted for this version to appear in e-Publications@Marquette. Elsevier does not grant permission for this article to be further copied/distributed or hosted elsewhere without the express permission from Elsevier.

Contents

Abstract 2
PACS ..... **Error! Bookmark not defined.**
Keywords 2
1. Introduction 3
2. Analytic equations 3
   2.1. Pull-in voltage 3
   2.2. Contact force 5
   2.3. Contact resistance 6
   2.4. Collapse voltage 6
3. Finite element modeling 7
4. Experiment 8
5. Results comparison 11
   5.1. Analytic predictions 11
   5.2. Finite element predictions 11
   5.3. Measurements 12
6. Conclusions 12
Acknowledgements 13

References 13

A comparison of micro-switch analytic, finite element, and experimental results

R. A. Coutu Jr.
Department of Electrical and Computer Engineering, Air Force Institute of Technology, Wright Patterson AFB, OH
P. E. Kladitis
Department of Electrical and Computer Engineering, Air Force Institute of Technology, Wright Patterson AFB, OH
L. A. Starman
Air Force Research Laboratory—Sensors Directorate, Hanscom AFB, MA
J. R. Reid
Air Force Research Laboratory—Sensors Directorate, Hanscom AFB, MA

Abstract
Electrostatically actuated, metal contact, micro-switches depend on having adequate contact force to achieve desired, low contact resistance. In this study, higher contact forces resulted from overdriving cantilever beam style switches, after pull-in or initial contact, until the beam collapsed onto the drive or actuation electrode. The difference between initial contact and beam collapse was defined as the useful contact force range. Micro-switch pull-in voltage, collapse voltage, and contact force predictions, modeled analytically and with the CoventorWare finite element software package, were compared to experimental results. Contact resistance was modeled analytically using Maxwellian spreading resistance theory. Contact resistance and contact force were further investigated by varying the width of the drive electrode. A minimum contact resistance of 0.26 Ω was measured on micro-switches with 150 µm-wide drive electrodes. The useful contact force range for these devices was between 22.7 and 58.3 V. Contributions of this work include: a contact force equation useful for initial micro-switch designs, a detailed pull-in voltage, collapse voltage, and contact force investigation using CoventorWare, a direct comparison of measured results with analytic and finite element predictions, and a means of choosing a micro-switch operating point for optimized contact resistance performance.

Keywords
MEMS; Micro-switch; Contact force; Contact resistance

1. Introduction

Analytic equations, finite element modeling (FEM), and simulation design tools are useful for evaluating microelectromechanical systems (MEMS) designs prior to device fabrication.[1] Previous micro-switch studies have focused on contact resistance models[2] and the impact of contaminant films.[3] In this study, the effects on contact force of overdriving cantilever-style, electrostatically actuated, micro-switches beyond the pull-in voltage were examined. Additionally, beam pull-in and collapse voltage predictions based on analytic equations and FEM were compared to measured values.

Analytic equations were used to predict pull-in voltage, collapse voltage, contact force, and contact resistance, while the CoventorWare[4] finite element software package was used to predict beam pull-in, collapse, and contact force. Measured pull-in, collapse, and contact resistance values were compared to the analytic and FEM predictions. Contact resistance and the useful contact force range were further investigated by varying the micro-switch's drive electrode width from 50 to 350 μm.

The cantilever-style switch, depicted in Fig. 1, is 75 μm-wide and 400 μm-long and the drive electrode width is a 150 μm-wide. The apparent contact area is defined by two upper contact dimple areas. Each dimple is approximately 8 μm in diameter and the contact metallurgy is gold-on-gold.

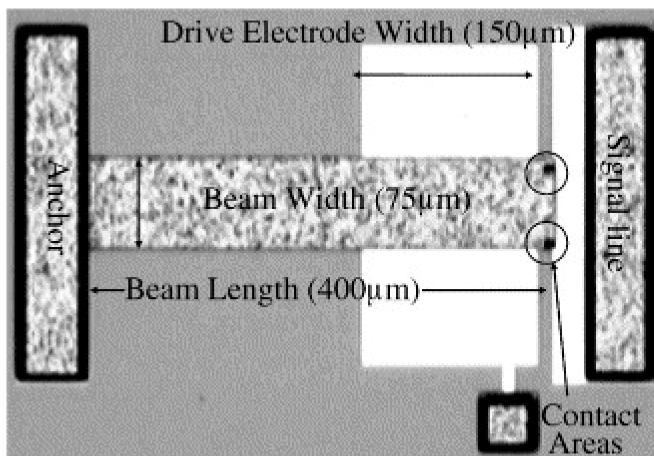

Fig. 1. A captured video image of a micro-switch, fabricated using a custom process similar to that in Table 1, with a 150 μm-wide drive electrode.

Simple models and analytic equations are useful micro-switch design tools for making initial predictions about device operation.

2. Analytic equations

Device pull-in voltage, contact force, contact resistance, and collapse voltage are modeled analytically in the following sections.

2.1. Pull-in voltage

Pull-in voltage is defined as the voltage at which the resulting electrostatic force overcomes the elastic restoring force of the cantilever beam and the switch snaps down. The device studied here, prior to pull-in, is assumed to behave like the beam illustrated by Fig. 2, with a fixed end at x=0, a free end at x=l, and an intermediately placed external load (F_a) at x=a.[5,6] Micro-switch pull-in, illustrated by the dashed line

in Fig. 2, is an important device parameter that defines the initial switch closure (when physical contact between the switch's upper (i.e. dimples) and lower electric contacts is first established).

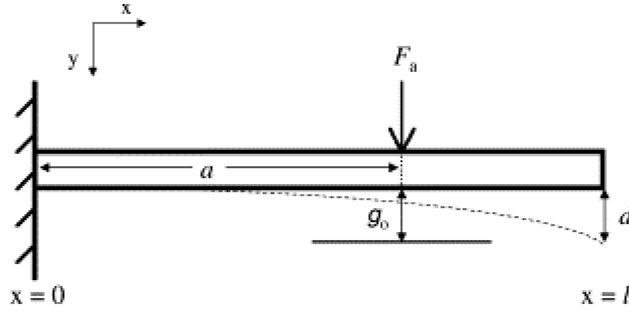

Fig. 2. Cantilever beam model with a fixed end at (*x*=0), a free end at (*x*=*l*), and an intermediately placed external load, F_a.

Eq. (1) is used to find maximum beam tip deflection with an intermediately placed load, located at the center of the switch's drive electrode:

(1)

$$d = F_a a^2 6EI_z(31 - a),$$

where *d* is the maximum tip deflection, F_a the applied load, *a* the load position, *l* the length of the beam, *E* the elastic modulus, and I_z the area moment of inertia about the *z*-axis.[6] The elastic modulus value used in this study was 80 Gpa.[7]

The applied load (F_a) is modeled as an electrostatic force:

(2)

$$F_e = \epsilon_o A_{sa} V^2 2g^2,$$

where, F_e is the electrostatic force, ϵ_o the permittivity of free space, A_{sa} the surface area of one parallel plate, *V* the actuation voltage, and *g* the gap between the plates.[7] F_e is represented by F_a on Fig. 2, Fig. 3.

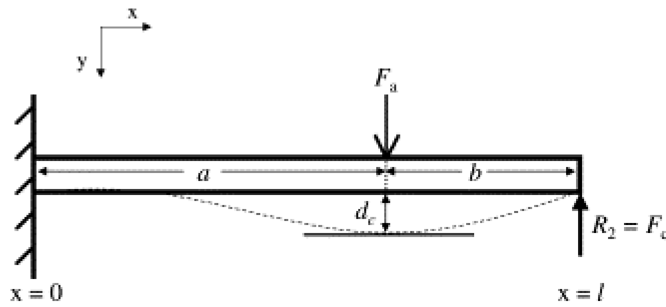

Fig. 3. Cantilever beam model with a fixed end at *x*=0, a simply supported end at *x*=*l*, and an intermediately placed external load (F_a) at *x*=*a*.

The beam's pull-in voltage is found using Eq. (3):

(3)

$$V_{pi} = (g_o - d_{pi}) 2k_1 d_{pi} \in_o A_{sa},$$

where V_{pi} is the pull-in voltage, (g_o−d_{pi}) the gap as the switch closes, k_1 the spring constant, and d_{pi} the pull-in distance.[7]

2.2. Contact force

When the pull-in voltage is applied and the beam snaps down, the switch's electric contacts are in physical contact with minimum contact force. The resulting contact resistance is usually too high for most applications.[5] Contact force can be increased (thereby decreasing contact resistance) by overdriving the device with increased actuation voltages above V_{pi}.

After pull-in, the switch is modeled as a beam with a fixed end at x=0, a simply supported end at x=l, and an intermediately place external load (F_a) at x=a as illustrated in Fig. 3.

Unlike the previous model, this new beam model is statically indeterminate and an additional equation is needed to supplement the static equilibrium equations (i.e. $\sum F_x=0, \sum F_y=0$, and $\sum M=0$). Using the principle of superposition, beam tip deflection in Fig. 3 is represented by the sum of two statically determinate systems. The first system is identical to Fig. 2 and the second is a beam with fixed end at x=0, a free end at x=l, and an end load (−R_2) at x=l. Eq. (4) is the resulting equation for maximum tip deflection for the second statically determinate system.[6]

(4)

$$d' = -R_2 l^3 3EI_z,$$

where d' is the maximum tip deflection and R_2 the applied force (N) at the beam's free end.

The final equation, needed to solve the indeterminate system shown in Fig. 3, is found by assuming zero tip deflection (i.e. zero deflection and no contact material deformation). Summing , , setting the sum equal to zero, and solving for the reaction force, R_2, results in:

(5)

$$R_2 = F_a a^2 21^3 (31 - a).$$

For micro-switches, the beam reaction force is equal to contact force and the applied load is equal to electrostatic force Eq. (2). Substituting F_c for R_2, Eq. (2) for F_a, and g=g_o−d, in Eq. (5) results in:

(6)

$$F_c = \in_o A_{sa} V^2 a^2 41^3 (g_o - d)^2 (31 - a).$$

Eq. (6) is used to determine switch contact force and is valid until the beam collapses onto the drive electrode. Switch contact resistance, discussed next, is another important device parameter that requires accurately modeled contact force.

2.3. Contact resistance

The resistance that results from closing a switch is defined by Eq. (7) which considers the effects of constriction (R_c) and contaminant film (R_{cf}) resistances:[8]

(7)

$$R_C = R_c + R_{cf}.$$

Constriction resistance, due to contacting surface topography, is modeled analytically using Maxwellian spreading resistance theory:[8]

(8)

$$R_c = p2r_{eff},$$

where R_c is the constriction resistance, ρ the resistivity, and r_{eff} the effective radius of a circular contact area.

Eq. (8) assumes that current flow is solely due to diffusive electron transport.[8] Unlike previous micro-contact resistance studies, the effects of ballistic electron transport[2] and contaminant film resistance[3] are not considered here.

When contact material deformation is assumed to be plastic, Eq. (8) is revised using Abbott and Firestone's material deformation model,[9] resulting in the well known Holm's contact resistance equation:

(9)

$$R_c = 0.886pHF_c,$$

where H is the contact material's hardness and F_c contact force.[8] The hardness and resistivity values used in this study for the gold electric contacts were 2 GPa and 2.2 μΩ cm, respectively.[8]

From Eq. (9), we know that contact resistance decreases as contact force or the applied actuation voltage increases. The limiting factor is when the collapse voltage is reached and the micro-switch fails.

2.4. Collapse voltage

The pulled-in beam's collapse voltage was found using:

(10)

$$V_{cpi} = g_1 - d_c a2k_2 d_c \in_o A_{sa,}$$

where V_{cpi} is the collapse voltage (V), d_c the collapse distance, k_2 the spring constant, and g_1 the initial gap under the beam depicted in Fig. 3. At collapse, illustrated by the dashed line in Fig. 3, physical contact between the cantilever beam and the drive electrode is established and the device shorts out. For comparison, the following section presents micro-switch pull-in voltage, contact force, and collapse voltage modeled and simulated using CoventorWare.

3. Finite element modeling

Finite element modeling and simulation are useful for detailed analysis of MEMS devices. The CoventorWare software packaged was used to model and simulate the micro-switches in this study (Fig. 4).

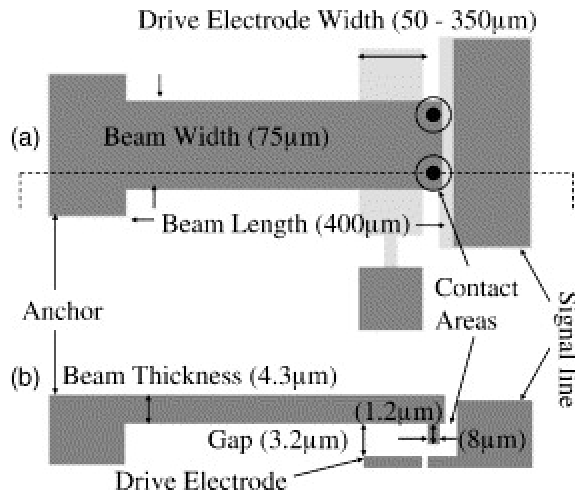

Fig. 4. Micro-switch layout: (a) top view; (b) side view.

After defining the foundry required by CoventorWare to construct the solid model (Table 1), the solid model was meshed using CoventorWare's "Free (tetrahedra)" and "Manhattan (brick)" elements. Tetrahedra elements were used to mesh the conformal geometry of the structural layer while brick elements were used to mesh the planarized geometry of the drive electrode and lower contact. These files, created separately, were combined into a single mesh prior to running each of the simulations. This procedure was used to provide the best overall nodal coverage of the device.

Table 1. Summary of the custom fabrication process and foundry defined in CoventorWare

Step	Action	Material	Layer/mask name	Thickness/depth (µm)
0	Base	GaAs	Substrate	20.0
1	Deposit	Gold	Lower contact	0.3
2	Deposit	Air dielectric	Dielectric	0.001
3	Etch		Electrode	0.301
4	Deposit	Photoresist	Sacrificial	3.2
5	Etch		Anchor/dimple	3.2/1.2
6	Deposit	Plated gold	Structural	4.3

A careful mesh analysis was accomplished to ensure accurate, timely simulation results. The process consisted of establishing realistic boundary conditions, meshing the solid model, and running a CoventorWare "pull-in" simulation. After each simulation, the number of nodes in the structural layer was compared to the resulting beam collapse voltage to determine if additional nodes were needed. Fig. 5 is an example of a CoventorWare simulation result where the beam has collapsed onto the drive electrode.

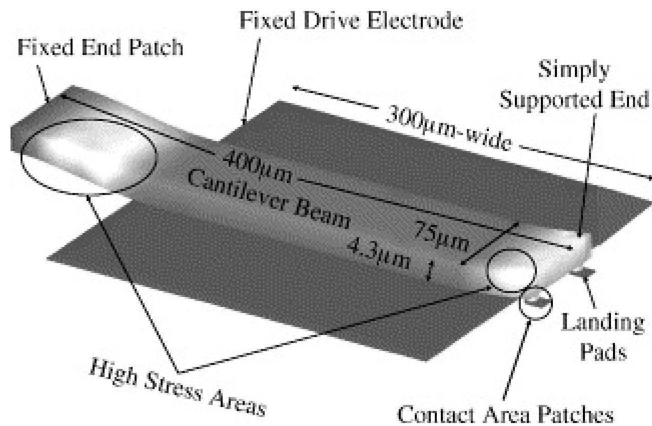

Fig. 5. CoventorWare simulation results for micro-switch stress with collapse voltage applied. The device has a 300 µm-wide drive electrode.

A dielectric layer (i.e. Air dielectric in Table 1), not present in the actual device, was defined on top of the drive electrode to avoid crashing the simulation upon reaching the beam's collapse voltage. Mesh analysis results (Fig. 6) show that structural layer meshes greater than approximately 650 nodes do not change the collapse voltage by more than 1 V. Structural layer meshes created with 664 mesh nodes were used for all the simulation data runs.

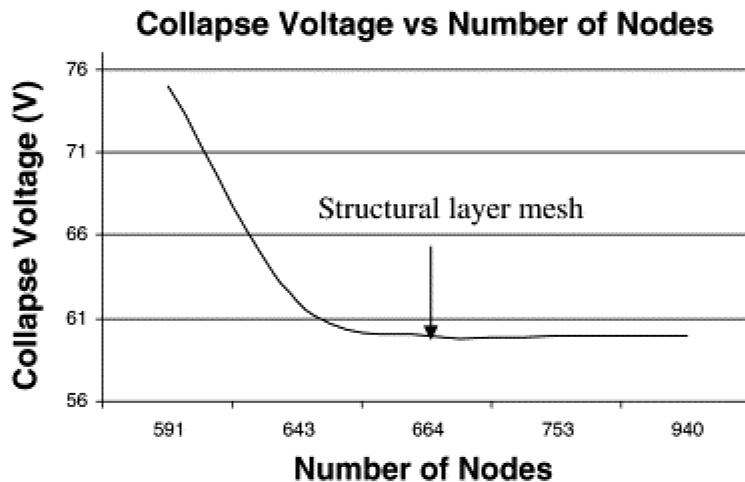

Fig. 6. Micro-switch mesh analysis results.

Once an adequate mesh size was defined, a full CoventorWare pull-in simulation was run with a voltage trajectory ranging from 0 to 75 V with one volt increments. The resulting output data file contained the switch's pull-in voltage, collapse voltage, and contact forces.

4. Experiment

A series of 75 µm-wide by 400 µm-long micro-switches (Fig. 1) were used to characterize pull-in voltage, collapse voltage and resistance. The devices were fabricated with drive electrode widths varying from 50 to 350 µm.

During operation a bias or actuation voltage was applied between the cantilever beam and the drive electrode. The metal contact switch closes when the magnitude of the bias voltage exceeds the pull-in voltage, V_{pi}. As the applied bias is increased beyond the pull-in voltage, the contact force increases and a second threshold is reached when the cantilever beam collapses onto the drive electrode at V_{cpi}. The maximum contact force is bounded by the maximum voltage that can be applied before the beam collapses. Once the second threshold is reached, the switch shorts out and is no longer operable. The voltage range between initial pull in and the collapse of the beam onto the drive electrode is the useful operating range of the switch:

(11)

$$V_{pi} \leq V < V_{cpi}.$$

The switches were tested by wafer probing using a Cascade Summit 9000 Microprobe Station with standard microprobes. The actuation voltage, applied using an HP 3245A universal source, was swept from 5 to 75 V in 1 V steps. Closed switch resistance was measured using an HP 34401A multimeter in a four-point probe configuration and beam deflections were measured using a Burleigh Horizon interferometric microscope (IFM). Fig. 7 is a schematic illustration of the experimental setup.

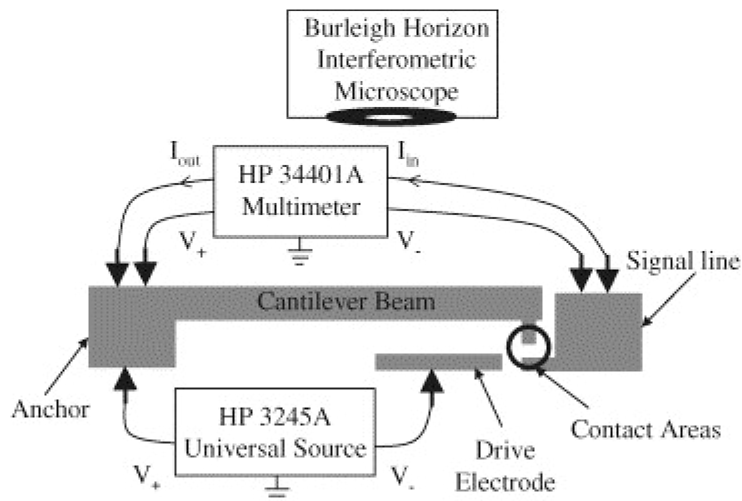

Fig. 7. Schematic illustration of the circuit used to actuate the micro-switches, measure the closed switch resistance, and determine beam deflection.

Fig. 8 shows the measured switch resistance as a function of the applied actuation voltage for one of the devices. At pull-in, the resistance drops when electrical contact is first initiated, while at collapse the measured resistance increases sharply indicating that the beam has collapsed onto the bottom electrode. Once pull-in is achieved, the resistance gradually decreases from approximately 3 Ω to approximately 0.300 Ω . The initial decrease in closed switch resistance is due to quasi-metallic contact and fritting or the pushing aside of resistive contaminant films as the contact force is increased [3]. As the contaminant films are fritted, metal-to-metal Ohmic contact areas also increase as the contact material plastically deforms resulting in decreased resistance.[8] Maximum contact force (minimum resistance) occurs just prior to the beam collapsing onto the bottom electrode. Once collapse occurs, the voltage drops to approximately zero and the resistance rapidly increases because of current flowing

from the drive electrode through the switch. This additional current corrupts the beam's four-point probe resistance measurement depicted in Fig. 7.

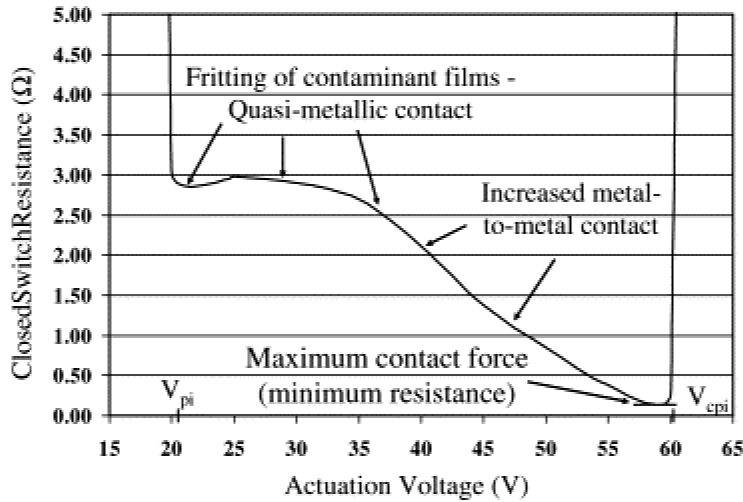

Fig. 8. Representative plot of measured switch resistance versus applied actuation voltage for a switch with a drive electrode 150 µm-wide. The initial drop in the measured resistance occurs at the pull-in voltage and sharp increase in resistance occurs at the collapse voltage.

To confirm that the measured voltage goes to zero due to beam collapse and not because of a surface breakdown current, an optical profile was taken of two switches (Fig. 9). The first switch was measured prior to any testing and the second was measured after it had been tested through collapse.

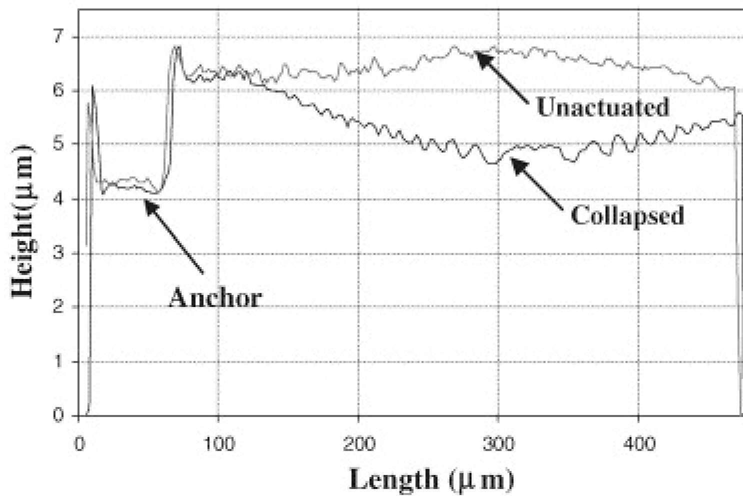

Fig. 9. Measured beam deflections obtained using an interferometric microscope illustrating the curvature of unactuated and collapsed cantilever beams.

The profiles, captured using the Burleigh Horizon interferometric microscope, show that the unactuated beam has a slight downward curl. This curvature follows the profile of the sacrificial layer that conforms to the underlying electrode layer. The beam that has been collapsed clearly shows an upward curvature with the lowest point over the drive electrode. This profile is consistent with the beam having collapsed

onto the bottom electrode. A comparison of analytic, finite element, and measured results is presented next.

5. Results comparison

5.1. Analytic predictions

Table 2 is a summary of the analytical-based pull-in voltage, collapse voltage, maximum contact force, and minimum contact resistance simulation results. The simulated pull-in and collapse voltages decrease as the drive electrode width increases. Also, the maximum contact force, defined as the force one volt prior to beam collapse, has a parabolic relationship with the drive electrode width. A maximum contact force of 45.4 µN was found, using Eq. (6), for devices with drive electrodes 150 µm-wide. The predicted useful contact force range lies between the pull-in (20.3 V) and collapse voltages (64.6 V). The minimum contact resistance, found using Eq. (9), was 0.13 Ω.

Table 2. Analytically calculated pull-in voltage, collapse voltage, maximum contact force, and minimum resistance for devices with drive electrodes ranging from 50 to 350 µm-wide

Width (µm)	**Pull-in (V)**	**Collapse (V)**	**Max. contact force (µN)**	**Min. contact resistance (Ω)**
50	31.4	>75	13.2	0.24
100	23.4	>75	27.3	0.16
150	20.3	64.6	45.4	0.13
200	18.8	46.9	27.9	0.16
250	18.1	37.7	18.8	0.20
300	18.0	32.8	14.2	0.23
350	18.3	30.3	11.7	0.25

5.2. Finite element predictions

Table 3 is a summary of the FEM-based pull-in voltage, collapse voltage, and maximum contact force simulation results produced using CoventorWare. Again, the simulated pull-in and collapse voltages decrease as the drive electrode width increases. A maximum contact force of 35.5 µN was found, using CoventorWare, for devices with drive electrodes 150 µm-wide. The corresponding predicted useful contact force range is between 21 and 66 V.

Table 3. CoventorWare simulation results for pull-in voltage, collapse voltage, and maximum contact force for devices with drive electrodes ranging from 50 to 350 µm-wide

Width (µm)	**Pull-in (V)**	**Collapse (V)**	**Max. contact force (µN)**
50	32	>75	11.0
100	24	>75	27.5
150	21	66	35.5
200	21	59	29.9
250	21	56	29.8
300	20	54	25.4
350	20	53	25.1

5.3. Measurements

Table 4 is a summary of the pull-in voltage, collapse voltage, minimum resistance, and contact resistance measurements. Contact resistance values were determined by subtracting the measured resistance of the beam (0.029 Ω) from the resistance values found using the experimental setup shown in Fig. 7. Measured pull-in and collapse voltages decrease as the drive electrode width is increased. Minimum resistance values were measured for devices with 100 and 150 µm-wide drive electrodes. The measured useful contact force range was between 24.3 and 61.0 V for devices with 100 µm-wide drive electrodes and between 22.7 and 58.3 V for devices with 150 µm-wide drive electrodes.

Table 4. Experimental pull-in voltage, collapse voltage, minimum resistance, and minimum contact resistance measurements for devices with drive electrodes ranging from 50 to 350 µm-wide

Width (µm)	Pull-in (V)	Collapse (V)	Min. resistance (Ω)	Min. contact resistance (Ω)
50	25.9	61.8	0.38	0.35
100	24.3	61.0	0.28	0.25
150	22.7	58.3	0.29	0.26
200	22.8	59.5	0.33	0.30
250	22.8	59.3	0.42	0.39
300	22.6	57.9	0.48	0.45
350	21.3	57.3	0.81	0.78

The FEM and analytically derived relationship between drive electrode width and pull-in voltage, shown in Table 2, Table 3, agree with the experimental pull-in voltage measurements found in Table 4. The collapse voltages found using CoventorWare (Table 3) agree with the collapse voltage measurements (Table 4). As the drive electrode width increases, however, the collapse voltages found using Eq. (10), agree less and less with CoventorWare or the measurements. Since the increased electrostatic force changes the shape of the beam, the model used in Fig. 3 becomes less accurate.

The CoventorWare and analytic contact force calculations have the same trend and both predict that maximum contact force is generated by overdriving switches with 150 µm-wide drive electrodes. The resistance measurements in Table 4 have a similar trend as the analytical resistance predictions in Table 2. Although, the resistance measurements for switches with 100 µm-wide drive electrodes were slightly lower than for devices with 150 µm-wide drive electrodes, the corresponding collapse voltages were higher. This indicates that more applied voltage was needed with 100 µm-wide devices than with the 150 µm-wide devices to generate the same contact force (and resulting contact resistance).

6. Conclusions

Electrostatically actuated, metal contact, micro-switches depend on having adequate contact force to achieve desired, low contact resistance.[2,3,8] Using analytic equations and CoventorWare, micro-switches were simulated and pull-in voltage, collapse voltage, and maximum contact force were predicted. Higher simulated contact force resulted from overdriving the cantilever beams after initial switch closure or pull-in. Experimentally, overdriving the cantilever beams, beyond the pull-in voltage, resulted in lower contact resistance measurements and therefore higher contact force values. The difference between pull-in voltage and beam collapse voltage was defined as the useful contact force operating

range. This operating range, depicted in Fig. 8, is useful for determining a specific operating point for micro-switch applications. For example, if closed switch resistance values of approximately 1 Ω are needed the micro-switches studied here should be operated at approximately 48 V.

The simulation results show that MEMS switches, with this geometry, and a 150 µm-wide actuation electrode, can achieve the highest contact force when overdriven and operated within the useful contact force range. Pull-in voltage, collapse voltage, and resistance measurements agree with simulated results obtained from analytic equations and CoventorWare. This agreement, between predictions and measurements, enables reliable fabrication of MEMS without wasting valuable wafer processing space.

Overall, analytic equations are useful for investigating initial micro-switch designs and FEM design tools are useful for accomplishing more detailed analysis prior to fabricating actual devices.[1] This approach to micro-switch design, modeling, and simulation will help maximize reliability and performance of fabricated devices. In addition, the simulations accomplished here show CoventorWare to be a useful software tool for evaluating micro-switch designs by predicting pull-in voltage, collapse voltage, and contact force.

Acknowledgements

This work was sponsored by the Materials and Manufacturing Directorate, Air Force Research Laboratory, USAF, under Project order number QGWSML02722002, POC: Dr. Robert L. Crane. The authors would also like to acknowledge the Sensors Directorate, Air Force Research Laboratory, in particular, Dr. Jack Ebel, Dr. Rick Strawser, Dr. Becky Cortez, and Dr. Kevin Leedy for developing the custom micro-switch fabrication process.

References

1. R. Sattler, *et al.* **Innovative design and modelling of a micromechanical relay with electrostatic actuation.** *J. Micromech. Microeng*, 11 (2001), pp. 428-433
2. S. Majumder, *et al.* **Study of contacts in an electrostactically actuated microswitch.** *Sens. Actuators A,* 93 (2001), pp. 19-26
3. D. Hyman, M. Mehregany. **Contact physics of gold microcontacts for MEMS switches.** *IEEE Trans. Comp. Packag. Technol*, 22 (1999), pp. 357-364
4. CoventorWare Inc., *Analyzer Ref. Guide*, http://www.coventor.com, 2001.
5. G. Rebeiz, *RF MEMS Theory, Design, and Technology*, John Wiley & Sons, Inc., New Jersey, 2003.
6. J. Shigley, C. Mischke, *Mechanical Engineering Design*, fifth ed., McGraw-Hill, New York, 1990.
7. G. Kovacs, *Micromachined Transducers Sourcebook*, McGraw-Hill, New York, 1998.
8. R. Holm, *Electric Contacts: Theory and Applications*, Springer, Berlin, 1969.
9. E. Abbot, F. Firestone. **Specifying surface quantity—a method based on the accurate measurement and comparison.** *ASME Mech. Eng*, 55 (1933), p. 569